Brain Multiphysics 5 (2023) 100082

Contents lists available at ScienceDirect

Brain Multiphysics

journal homepage: www.sciencedirect.com/journal/brain-multiphysics

Research article

Modal analysis of computational human brain dynamics during helmeted impacts

Fargol Rezayaraghi [a], Javid Abderezaei [a], Efe Ozkaya [b], Devlin Stein [c], Aymeric Pionteck [a], Mehmet Kurt [a,b,*]

[a] *Department of Mechanical Engineering, University of Washington, WA, USA*
[b] *BioMedical Engineering and Imaging Institute, Icahn School of Medicine at Mount Sinai, New York, NY, USA*
[c] *Department of Biomedical Engineering, Stevens Institute of Technology, Hoboken, NJ, USA*

ARTICLE INFO

Keywords:
Brain biomechanics
Helmet design
Modal analysis
Sport helmet
Traumatic brain injury

ABSTRACT

Sports-related mild traumatic brain injury (mTBI) is a growing public health concern, affecting millions in the U.S., annually. Current helmets are primarily designed to mitigate head kinematics, despite the importance of the brain substructures mechanics in mTBI mechanism. Therefore, it is crucial to consider the dynamical behavior of brain substructures, which has been shown in prior studies to be associated with strain concentration. Here, we studied the modal behavior and strain patterns of the substructures of the brain finite element (FE) model through Dynamic Mode Decomposition. We conducted side and front impact pendulum tests on a dummy headform equipped with hockey, football, ski, and bicycle helmets. After simulating the impact tests using a brain FE model, we calculated the dynamic modes of this computational model for the whole brain, corpus callosum, brainstem, and cerebellum. The main mode of oscillation in all regions for all helmet types occurred around the frequency regime of 7–15 Hz. Also, in cerebellum, a second harmonic was observed at 40–50 Hz in front impact, and 38 and 62 Hz in side impact in bicycle and ski helmets, respectively. Furthermore, we analyzed the correlation between the modal response and peak maximum principal strain (MPS). These analyses mostly showed a direct association between the computational modal behavior and MPS, where helmet tests with closely spaced modes and high-frequency modal amplitudes led to higher MPS values. This association between the computational modal behavior and strain patterns demonstrated a potential for improving helmet designs through a novel design objective.

Statement of significance: Sport-related mild traumatic brain injury (mTBI), which is one of the leading cause of death, can be reduced in severity by using headgears including helmets. Despite the recent innovations and technologies in helmet design, there are important factors that still have been missed. While it's been shown that the brain substructures mechanics play an important role in mTBI mechanism, current helmets are designed to only mitigate the head kinematics. Moreover, dynamical behavior of these substructures, and existence of multimodal behavior in the brain are factors that have not been addressed in designing helmets. This paper shows the effect of different helmet types on modal behavior of the brain substructures and how the dynamical modes of these regions can be affected by using various helmet types.

1. Introduction

Traumatic brain injury (TBI) is one of the main causes of death and disability worldwide [1]. Mild TBI (mTBI), and more specifically sport-related mTBI, risks the health of hundreds of thousands of athletes every year [2,3], leading to, in certain cases, long term disability and neurocognitive deficits [4]. Helmets have been used in several contact sports as a protection strategy to prevent or reduce the severity of mTBI. Although helmets have been shown to significantly reduce the risks of severe head injuries in football [5], bicycling [6,7], skiing [8], and other sports, their effectiveness in mitigating the risks of milder forms of TBI is still being investigated [9–11].

Sports helmets have different shapes, mechanical properties, and testing criteria based on the particular contact sport [12–15]. Football and hockey helmets have usually hard shells and thicker but softer liners that are made up of polyurethane (PU) and vinyl nitrate (VN) foams [5,12,13,16]. On the other hand, bicycle and ski helmet liners

* Corresponding author.
E-mail addresses: fargor@uw.edu (F. Rezayaraghi), mkurt@uw.edu (M. Kurt).

https://doi.org/10.1016/j.brain.2023.100082
Received 22 December 2022; Received in revised form 16 May 2023; Accepted 14 August 2023
Available online 22 August 2023

typically consist of Expanded polystyrene (EPS) [14,15] foam. The safety performance of the helmets is generally evaluated using the kinematics of the head using a form of laboratory impact setup [17–19]. Hockey and football helmets are typically tested with setups that include rotational kinematics, such as an impact pendulum device [20] and a horizontal impactor [21]. Ski and bicycle helmets have been traditionally tested and evaluated with a vertical drop-test setup for linear kinematics. The criteria that helmets should pass during testing procedure, might vary among different standards that were introduced for various sports helmets. For instance, bicycle helmets impact performance standards are determined by Consumer Protection Safety Commission (CPSC) [19,22], and football helmet standards are set by National Operating Committee on Standards for Athletic Equipment (NOCSAE) [23]. The conventional helmet design framework considers the paradigm that the linear kinematics of the head during an impact should be reduced [17,24]. Due to the growing evidence of the rotational head kinematics' role in head injuries and the evidence that rotation-induced brain strain plays an important role in concussion mechanism [25–33], novel helmet designs have been proposed to reduce head rotation. These findings encouraged incorporating the importance of mitigating the rotational kinematics in the helmet testing standards [27,34] and evaluation of various helmet types [20,27,35,36]. Preliminary experimental studies [19,37] along with computational simulations [37] demonstrate that these mitigation systems reduce rotational kinematics and the brain strain [7]. Despite these recent improvements in the helmet designs, mTBI continues to have high incidence rates across different contact sports [29,38], which further signifies the need for better helmet designs, testing criteria, and design framework. Elucidating the mechanisms of brain injury is one of the substantial perspectives that can significantly reveal missing elements in designing more effective helmets.

To better understand the physical mechanism of mTBI, researchers have studied brain mechanics and deformation during impacts, by collecting human head impacts data [39–43] and/or by simulating impact scenarios with detailed computational models of the brain–skull system [39–48]. More specifically, anatomically-detailed finite element (FE) models of the human brain–skull system are commonly used in understanding the biomechanics of TBI, as they allow for the investigation of how the brain responds to external forces or stimuli [27,39–49]. Using detailed FE models of the human brain, studies have shown that peak principal strain in the brain correlated with injury diagnosis in various contact sports [43,50]. Therefore, in addition to traditional helmet testing and evaluation methods that study the rotational and linear kinematics of the head [7,35,37,51–59], researchers have also proposed investigating the mechanical behavior of the brain, which is closely correlated to the rotational kinematics of the head during impacts. This approach offers valuable insights into the effectiveness of helmets and enhances our understanding of how helmets can mitigate head injuries in impact scenarios [20,27,35,36].

Apart from analyzing the brain deformation as a brain injury metric, spatial and temporal variations in brain deformation characteristics have been hypothesized to have injury-related implications [49,60–63]. Studying the mechanical behavior of the human brain tissue through imaging techniques [64–68], computational simulations [69–71], and analyzing the mechanical impacts to the human brain [39,70] has demonstrated that certain regions, specifically periventricular regions such as corpus callosum (CC) experience strain concentrations [70,72], localized vibration modes [70], and higher strains [39,69,71] during impacts. In summary, as a result of a force impulse to the head, it is hypothesized that the shear waves inside the brain propagate and attenuate differently in various regions [70,73] which makes some regions such as white matter and CC more vulnerable to injuries [74]. These shear waves can cause a localized strain concentration [70,72] at certain regions such as the brainstem [73] and CC [70]. The pattern of these shear waves hypothetically is affected by rigid structures such as stiff ventricular or membranous structures in the brain [63,75]. For instance in a study by Abderezaei et al. in which they used WHIM brain FE model, it was observed that brain behaves nonlinearly during impacts, especially around the deep white matter [72]. Investigating the biomechanics of the substructures of the brain FE models such as KTH [70] and Worcester Head Injury Model (WHIM) [72] during impacts has also revealed crucial frequency-dependent and localized phenomena that have been associated with the injury outcome [70,72]. In another study, the frequency response of the human brain was investigated by identifying the natural modes and frequencies of three-dimensional (3D) deformation in vivo. Tagged magnetic resonance images (MRI) were acquired during transient mild acceleration of the head and 3D strain fields were analyzed using dynamic mode decomposition (DMD) [76]. Estimating strain fields that were representing dynamic, 3D brain deformations, revealed fundamental oscillatory modes of deformation at damped frequencies near 7 Hz in neck rotation and 11 Hz in neck extension [76]. Using DMD technique with KTH [70] and WHIM [72] FE model simulations showed the existence of distinct modal frequencies in the CC, and a strain concentration in deep regions of the white matter [70,72]. Specifically, the brain's behavior in computer models has been shown to be sensitive to displacement frequencies around 20–30 Hz, which exacerbated the observed deformation [70,72]. Moreover, investigating the frequency response of the brain model's substructures during an impact showed that the CC experiences a higher deformation at certain frequencies, with potential mTBI implications [70].

Considering the vulnerability of certain substructures of the brain (*e.g.* CC), and the existence of the multimodal and localized behavior which might cause strain concentration in these regions, there is a need to investigate the effect of different helmet designs on the frequency response of the brain structures. Studies that have investigated helmet performance and its role in reducing the severity of brain injury mostly have focused on the motion of the head and its kinematics [19,57], rather than the substructural mechanics of the brain tissue. One reason might be the complexity of the system which makes it computationally exhaustive to optimize the helmets based on large-scale computational models. Although attempts have been made to analyze the efficacy of the helmet types by looking into brain strain levels during an impact, a design optimization has not been proposed yet. Moreover, investigating the strain level of the brain tissue itself is crucial but not adequate enough to reach a comprehensive insight into the helmet's role in the brain injury mechanism. Substructural mechanics of the brain is another factor that needs to be considered, since analyzing the brain injury based on the regional-dependent strain criteria has shown a correlation between concussion diagnosis and maximum principal strain [77,78]. This vulnerability has brought specific attention to certain regions of the brain in sport-related concussion studies [79,80].

In this study, our purpose was to evaluate the effect of different helmets on the frequency response of the substructures of a brain FE model called Global Human Body Models Consortium (GHBMC). We performed impact pendulum tests on football, hockey, ski, and bicycle helmets, and by using the extracted kinematics from the helmeted dummy headforms, we simulated the tests in an FE brain-skull model. Using the DMD technique, we analyzed the frequency response of the substructures of the brain FE model across different helmet types. The final results provided insights into ways to improve the sports helmet designs by considering the computational dynamical behavior of brain.

2. Methods

In this study, first, we performed impact pendulum tests on helmeted headforms. Then, we simulated a computational model of the brain–skull system using the experimental head kinematics. Finally, we employed an advanced modal analysis technique to study the effect of different sports helmets on the frequency response of the brain substructures in the computational model (Fig. 1).

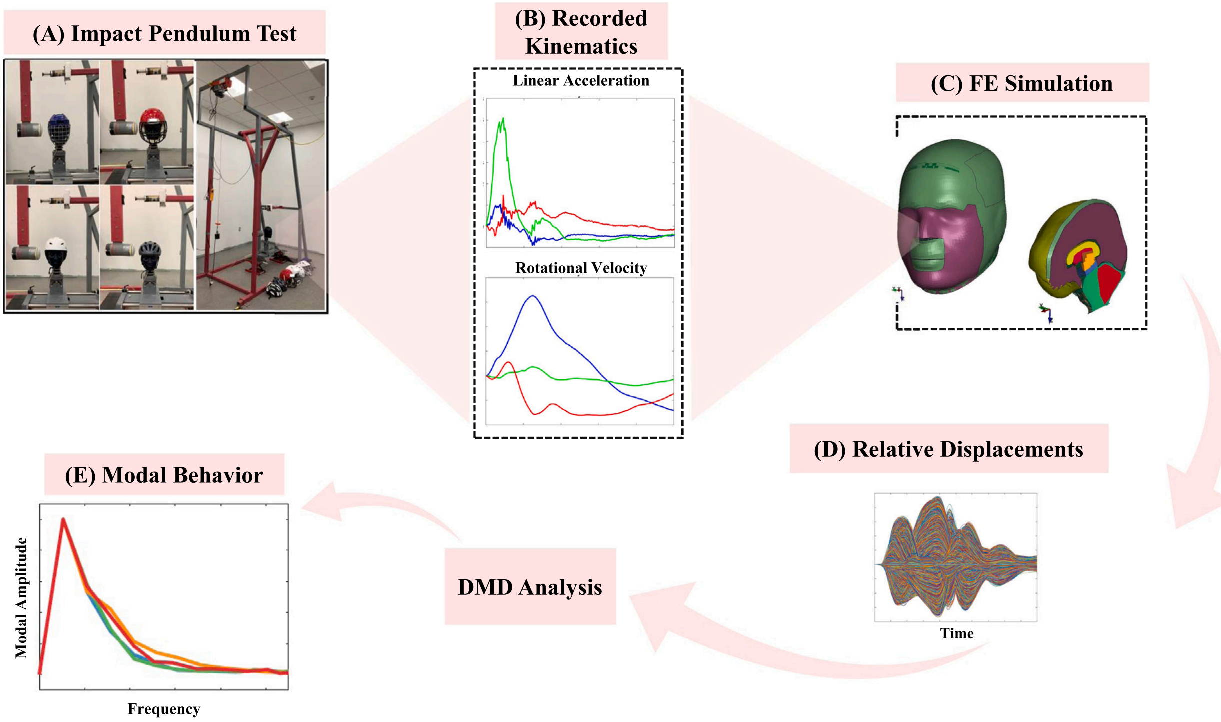

Fig. 1. Overview of the proposed helmet performance analysis. (A) We used a custom impact pendulum test setup to perform impact tests on hockey (top left), football (top right), ski (bottom left), and bicycle (bottom right) helmets. (B) Recorded linear acceleration and rotational velocity datasets were captured by the sensors located in the center of gravity of the dummy headform to be used in the subsequent FE analysis. (C) GHBMC brain FE model was used to simulate the impact scenarios. (D) Relative displacements were calculated in three anatomical planes for each region. (E) Dynamic mode decomposition (DMD) technique was used to analyze the modal response of the brain and its substructures.

2.1. Impact pendulum tests

We used an impact pendulum test setup to apply impacts to a Hybrid III anthropomorphic head-neck system (Fig. 1 A). We released the impact pendulum at a 60° angle, which corresponds to an impact velocity of 4.3 m/s. Four different commercially available helmets including a hockey helmet, a football helmet, a ski helmet, and a bike helmet (Fig. 1 A) were tested three times to compare their performance in mitigating the head kinematics, and the resultant dynamic response of the brain FE model. Hockey and football helmets that were tested had VN liner foams [12,16], and ski and bicycle helmet liners consisted of EPS foam [14,15]. Head kinematics were measured using a 6DOF sensor package (DTS, Seal Beach, CA), consisting of one tri-axial accelerometer (ACC3 PRO) and three angular rate sensors (ARS PRO-8K 2000 Hz), which were located at the center of gravity (CoG) of the dummy headform. We applied side impacts to induce coronal rotation since it has been reported that rotations in the coronal direction can cause large strains in certain vulnerable regions such as CC [69,81]. We also performed front impact tests in order to understand the directional dependence of the brain FE model's frequency response.

2.2. Finite element simulations

In order to simulate head impacts in LS-Dyna environment, we utilized the GHBMC 50th percentile male skull–brain FE model [82]. GHBMC is a computational model developed to simulate and study the biomechanics of human body movements and interactions with external forces, such as those experienced during automotive crashes [83–85]. This head model was developed based on CT and MRI scans of an adult male of average height and weight in the US [83]. The model's robustness was tested against 35 experimental head impact cases, with validation against brain pressure [86,87] and motion [88,89] data, facial [90] and skull bone [91,92] responses, and skull–brain motion [83]. The version we used for this study (version 5.1.1) consisted of two primary parts: the brain and skull, each of which comprised several components, with a total of 189,780 nodes and 244,485 elements. We applied linear acceleration and rotational velocity from impact pendulum tests to the center of gravity (CoG) of the head model. The purpose of the described tests and simulations was to observe the effect of different helmets on the dynamic response of the brain substructures in the computational model. We extracted nodal coordinates of the brainstem, CC, cerebellum, and the whole brain in three directions. Then, we calculated the relative displacement of each node at each region with respect to the skull. These calculated relative displacements were then used as inputs for the DMD analysis.

2.3. Modal analysis

DMD is a multivariate method that we used for extracting the modal behavior of the brain tissue, 1which allows for analyzing the spatiotemporal differences within the brain substructures as a function of modal frequency [70,76,93,94]. If we consider N equally spaced snapshots of a dynamic brain system that has M nodes, by considering the temporal sequence of the brain's nodal displacement in x, y, and z directions, we can write down the displacement fields at time t as:

$$\mathcal{U}(x, y, z, t) = \sum_{n=1}^{N} a_n exp(\lambda_n t)\phi_n(x, y, z) \tag{1}$$

where, a_n is the modal coefficient, λ_n is the complex modulus, and ϕ_n is the spatial distribution of each mode. As explained above, N is the number of spaced snapshots of M nodes, where each snapshot in DMD is assumed as a linear combination of the previous snapshots, $u_{j+1} = Au_j$ and can be written as:

$$\mathcal{U}_1^N = u_1, Au_1, \dots, A^{N-1}u_1 \tag{2}$$

By calculating the eigenvalues and eigenvectors of matrix A, which defines the dynamical process, we can find the frequency [ω_j =

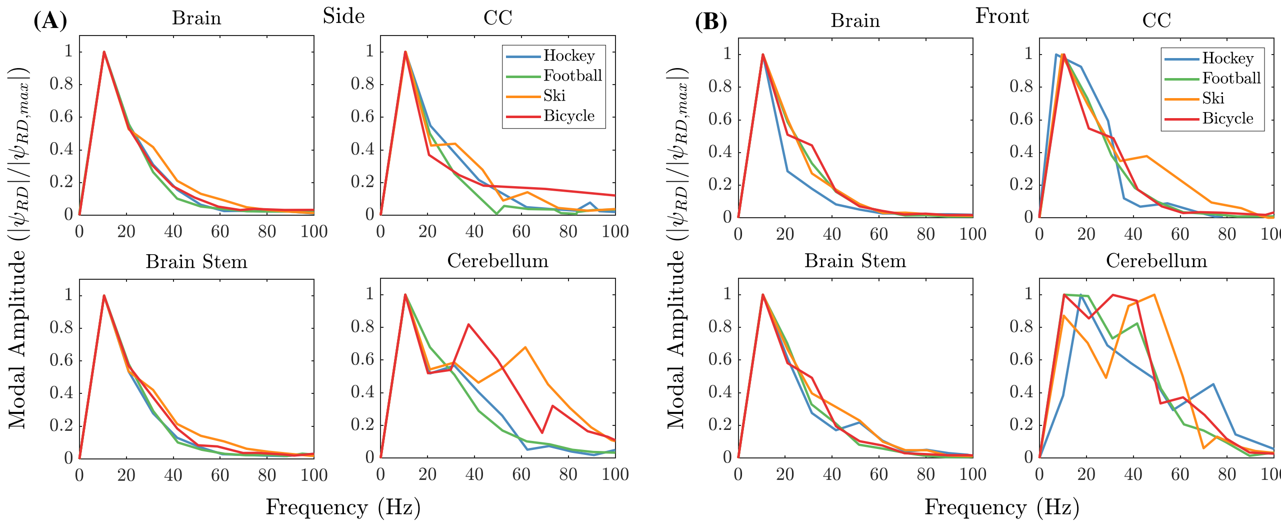

Fig. 2. Comparison of DMD modes in different subregions of the simulated brain model across different impact directions and helmets using brain–skull relative displacements. Normalized modal amplitudes in the brain, CC, brainstem, and cerebellum for different helmets in (A) side and (B) front impact directions. The first harmonic in all regions was around 7.1–15.5 Hz for both impact directions. (B). Cerebellum demonstrated a high-bandwidth modal response, with dominant high-frequency modes of oscillation observed in both impact directions.

Re(λ_n)], decay rate [$\zeta_j = \mathrm{Im}(\lambda_n)$], and amplitude ($|\Psi_j|$) of the dynamic modes [70].

To get a more extensive understanding of how different helmet types can affect the amplitude pattern of the modes in the brain regions, we did a secondary analysis. We defined a term called *cumulative amplitude* as a summation of the amplitudes in a desired frequency range. Since it has been shown that the brain has a multimodal behavior [70,72], the dominant frequency of the brain was considered as a reference frequency, ω_{ref}. We defined two frequency intervals and termed them as: low frequency range (ω_L), and high frequency range (ω_H) as (Eq. (3)):

$$\omega = \begin{cases} \omega_{\text{L}} & 0 \le \omega \le 2 \times \omega_{\text{ref}} \\ \omega_{\text{ref}} & \omega \text{ of the brain dominant harmonic} \\ \omega_{\text{H}} & 2 \times \omega_{\text{ref}} < \omega \end{cases} \tag{3}$$

In each case, we calculated the cumulative amplitude by summing up the amplitudes of the frequencies in low ω_L and high frequency range ω_H (Eq. (4)), separately:

$$\begin{aligned} |\Psi_{\omega_{\text{Sum}}}| &= \sum_{i=1}^{N} |\Psi_i|, \\ |\Psi_{\omega_{\text{L}}}| = \sum_{i=1}^{N_L} |\Psi_i|, \quad |\Psi_{\omega_{\text{H}}}| &= \sum_{i=1}^{N_H} |\Psi_i| \end{aligned} \tag{4}$$

where $\Psi_{\omega_{Sum}}$ is the sum of the all mode amplitudes, and N_L and N_H are the indices of the frequencies which are in the range of ω_L, and ω_H, respectively.

Our goal was to compare the performance of the helmets in reducing modal amplitudes, or in other words, dissipating energy in different frequency regimes. For a more accurate comparison of the cumulative amplitude distribution among low and high frequency ranges, we calculated the percentage of the low frequency and high-frequency cumulative amplitudes to the whole cumulative amplitude, separately. This analysis clarified how various helmets can affect the DMD modes and shift the percentage of energy in certain dominant bandwidths. By way of illustration, this analysis indicated what percentage of energy is dissipated in high or low frequency regimes and how the type of the helmet can affect this behavior.

To confirm the accuracy and reliability of our modal analysis results regarding the relative displacements, we performed a complementary modal analysis using the maximum principal strain (MPS) values of the individual elements within each brain region. Using MPS values for DMD technique was important since strain has been shown as an important indicator of injury in mTBI studies [80,81]. We followed the same procedures used for the previous analysis, which involved applying DMD on the relative displacements (Eqs. (1) and (2)). By incorporating MPS values in our modal analysis, we were able to obtain a more comprehensive understanding of the dynamical behavior of the brain FE model during helmeted impacts. Furthermore, this approach allowed us to establish a correlation between the modal characteristics of the relative displacements and the corresponding MPS values, thereby strengthening the validity of our modal analysis method.

2.4. Strain analysis

Strain has been shown to be a potential indicator of mTBI [69,95,96], and therefore analyzing the maximum principal strain (MPS) is one of the main parameters in understanding the physical basis of injury [97]. Here, in order to check the effect of mode localization on the brain strain, we considered CC, brainstem, and cerebellum, and calculated the ratio of the peak MPS in each region with respect to the peak MPS in the whole brain ($\frac{\text{MPS}^{\text{peak}}_{\text{subregion}}}{\text{MPS}^{\text{peak}}_{\text{Brain}}}$). Our purpose was to compare this metric with modal parameters and analyze them with respect to the helmet type.

3. Results

3.1. Frequency response of the brain subregions with helmeted impacts

We conducted DMD analysis using the brain–skull relative displacement on all four regions of the brain model as well as the whole brain for all the helmet types in both side (Fig. 2A and Fig. 3A) and front (Fig. 2B and Fig. 3B) impact directions. While the main harmonic for most regions for both side and front impacts was around 7–15 Hz, some outliers were observed in this computer model. Overall, CC and cerebellum demonstrated more deviance from the whole brain dynamics. In the front impacts for CC, the first harmonic occurred at 23.1 Hz in the bicycle helmet, with a more broadband spectrum observed for other helmets compared to the whole brain. Cerebellum

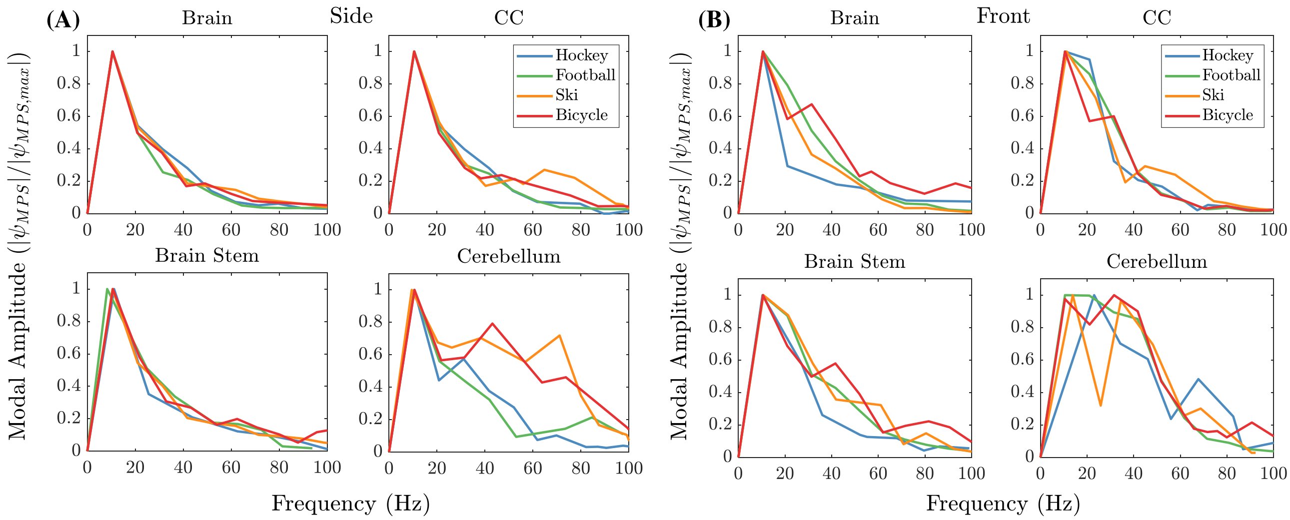

Fig. 3. Comparison of DMD modes in different subregions of the simulated brain model across different impact directions and helmets using MPS. Normalized modal amplitudes in the brain, CC, brainstem, and cerebellum for different helmets in (A) side and (B) front impact directions. The first harmonic in all regions was around 8.2–13.8 Hz for both impact directions. (B). Cerebellum demonstrated a high-bandwidth modal response, with dominant high-frequency modes of oscillation observed in both impact directions.

demonstrated a high-bandwidth modal response, with dominant high-frequency modes of oscillation observed in both impact directions. For instance, in side impacts, a dominant second modal peak appeared in bicycle and ski helmets around 37.5 Hz and 61.7 Hz, respectively (Fig. 2A). The occurrence of this dominant second modal peak in front impacts was at frequencies of 41.6, 31.3, and 38.0 Hz, in the football, bicycle, and ski helmets, respectively (Fig. 2B).

As detailed in the methods section, we validated our relative displacement-based modal analysis results by comparing them to the findings obtained through modal analysis of the maximum principal strain. Our analysis demonstrates a high degree of similarity between the two sets of results, with identical frequencies observed for the main harmonic and a close frequency range observed for the secondary harmonics. The predominant mode of oscillation was observed in the frequency range of 7–15 Hz for most regions in the majority of cases. The cerebellum exhibited a wide-band modal response, characterized by dominant high-frequency modes of oscillation in both impact directions. In side impacts, a dominant second modal peak was observed at frequencies of 43.1 Hz and 71.1 Hz in bicycle and ski helmets, respectively (Fig. 3A). For front impacts, the occurrence of this dominant second modal peak was at frequencies of 36.6 Hz, 36.7 Hz, and 41.4 Hz in football, bicycle, and ski helmets, respectively (Fig. 3B). Furthermore, we identified the presence of the second harmonic in specific cases, providing further evidence for the consistency and reliability of our findings. Our evaluation of the comparative bandwidth modal response across different helmet types and regions demonstrates a high level of consistency between the two modal analysis approaches. Additionally, we observed the presence of the second harmonic in specific cases, further supporting the consistency and reliability of our findings. Our examination of the comparative bandwidth modal response among different helmet types at each region shows that the results are also highly consistent between the two modal analysis approaches (Fig. 2 and Fig. 3).

A critical observation in the modal responses of different helmets was the difference in the frequency distribution of modes in different brain substructures (Fig. 2). Due to these differences in the amplitude distribution of modes in the frequency domain for different helmets, we binned the modes in two main frequency intervals (ω_L and ω_H in Eq. (3)) and estimated their cumulative amplitude percentage distribution. This analysis helped us understand the dominant frequency regimes for brain modes in different helmets and impact conditions. Comparing the cumulative amplitudes in the side impacts in the brain and brainstem showed that for high-frequency regime (which were shown as a solid color in Fig. 4), hockey (26.9%) and football (29.9%) helmets had lower cumulative amplitudes than the bicycle (34.2%) and ski helmets (40.9%). In the CC, the high-frequency cumulative amplitude in the football helmet was the lowest in side impacts (29.9%). In the cerebellum, the high-frequency cumulative amplitude of the football helmet was also the lowest (43.4%). Similar cumulative amplitude behaviors were observed in the hockey, the bicycle, and ski helmets for side impacts in cerebellum (Fig. 4A).

In the front impact, the high-frequency cumulative amplitude in the brain was the lowest in the hockey helmet (26.0%) and was the highest in the bicycle helmet (35.4%). No significant differences were observed between the ski and football helmets (29.2%). Also in the brainstem, the football helmet had the lowest (30.7%) and the ski helmet had the highest value for high-frequency cumulative amplitude (41.5%). In the CC, the high-frequency cumulative amplitudes were the lowest for football (30.3%) and hockey helmets (32.4%). In the cerebellum, which had more higher-amplitude modes in the higher frequency regimes compared to the other brain substructures, hockey helmet (66.8%) and ski helmet (66.7%) demonstrated the highest concentration of modes in the high-frequency regime (Fig. 4B).

3.2. Peak MPS pattern among brain subregions

Based on prior studies demonstrating the importance of brain's modal behavior during impacts in understanding the physical mechanism of injury [49,70,72,76,98], we studied the relationship between the brain's modes and strain responses of a brain computer model in the helmeted impacts. We hypothesized that modal coupling and higher modal density could result in energy localization of the brain that can exacerbate the effects of strain and subsequently, the risk of injury.

In this computer model, we analyzed the peak MPS in three brain regions including CC, brainstem, and cerebellum (Fig. 5). We specifically studied the ratio of the peak MPS in these regions with respect to the peak MPS in the whole brain ($\frac{\mathrm{MPS}^{\mathrm{peak}}_{\mathrm{subregion}}}{\mathrm{MPS}^{\mathrm{peak}}_{\mathrm{Brain}}}$) in order to study the strain localization patterns. The first observation was about the differences in the regions in which the highest ratio occurs in the side and front impact directions. In the side impacts, the highest ratio occurred in the CC for all the helmet types except the ski helmet. This ratio for the ski helmet in CC was 0.97, which did not have a substantial difference with other helmets (Fig. 5 Side). In the front impacts, the brainstem experiences the highest ratio among other regions of interest (Fig. 5 Front). This observation is in line with the previous studies in

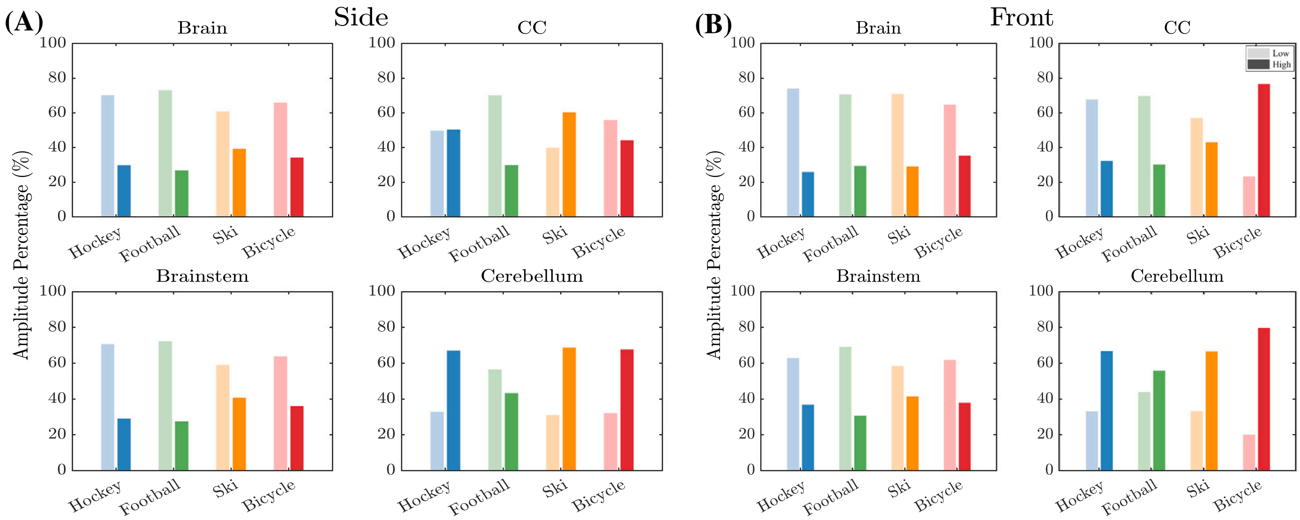

Fig. 4. Distribution of the DMD modes in low and high frequency ranges. This figure makes a comparison between the percentage of the cumulative modal amplitudes in the frequency ranges of ω_L and ω_H in the brain, CC, brainstem, and cerebellum in (A) Side and (B) Front impacts. A) In the high frequency range, the amplitude percentage was higher in the ski and bicycle helmets in the brain, and brainstem, compared to the hockey and football helmets. In the CC and cerebellum, football helmet had the lowest amplitude percentage in the high frequency range. (B) In the brain, CC, and brainstem, hockey and football helmets had the lowest amplitude percentage in the high frequency range. In the cerebellum, the amplitude percentage of the football helmet was the lowest in the high frequency range. (For interpretation of the references to color in this figure legend, the reader is referred to the web version of this article.)

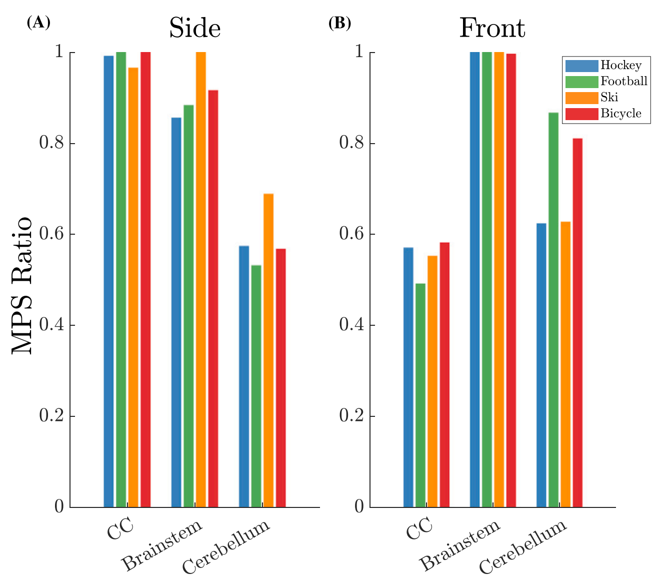

Fig. 5. Regional pattern of the peak MPS with respect to the peak MPS in the brain. This figure shows the ratio of the peak MPS in CC, brainstem, and cerebellum with respect to the peak MPS in the brain in (A) Side and (B) Front impacts. (A) In the side impact direction, the peak MPS occurs in CC for all helmet types, except ski helmet in which the peak MPS appears in the brainstem, but the difference between these two regions was negligible. Cerebellum has the lowest ratio compared to the other two regions. (B) In the front impact direction, the brainstem and CC have the highest and lowest ratio in all helmet types.

which the highest strain varies depending on the rotation plane [98–100]. Moreover, CC and brainstem which have the highest peak MPS ratio in our observations were found as regions that experienced large strains attributable to their surrounding stiff membranous structures, in previous studies [98,99,101]. A critical observation was about the helmet that experienced the highest peak MPS ratio in each region. In side impacts, ski helmet had the highest MPS ratio in both brainstem and cerebellum. Also, football helmet experienced the lowest MPS ratio in cerebellum in the side impacts. On the other hand, in the front impact, football helmet showed the highest MPS ratio in the cerebellum, and the lowest MPS ratio in CC.

4. Discussion

In most contact sports, athletes wear protective head gears to reduce the potential risks of head injuries. However, despite the recent advancements in helmet technology and increased use of helmets [56,102,103], the incidence rate of sports-related mTBI is still high, which necessitates further improvement of sports helmets. In spite of the increasing evidence about the role that the spatiotemporal mechanics of the brain substructures play during mTBI, current helmets are primarily designed by focusing on mitigating the head kinematics. The existence of the localized modes in the brain along with the multimodal behavior among the brain regions, and the vulnerability of the specific regions to injury, demonstrate the necessity to investigate the modal behavior of the brain substructures in helmeted impacts.

In this study, we identified differences in the model-predicted modal behavior of the subregions of the brain FE model, in the helmeted impacts by using the helmets of the sports with the most common injury rates. In all regions of the brain model, the main mode of oscillation was identified to be between the frequency regime of 7–15 Hz in both impact directions. The range of the main harmonics in this brain model and its structures aligns with the reported findings in prior studies [49,76]. These studies identified the dominant oscillatory modes of deformation as 7 Hz in neck rotation and 11 Hz in neck extension using tagged MRI [76], and 15–20 Hz through simulation of impacts coupled with measurements extracted from tagged MRI [49]. However, in some cases, the discrepancies can be anticipated due to variations in the tested regions across different experiments, as well as inherent differences between in-vivo [76] and computer-simulated results [49]. In the cerebellum, additional higher harmonics showed up in both impact directions. Depending on the impact direction and the helmet's type, a second high-amplitude mode oscillates in the frequency range of 38–62 Hz. This second oscillation mode in the cerebellum was also previously reported at the same frequency range [70,104]. This observation was due to higher frequency multimodal dynamics in the cerebellum [70]. Cerebellum is located at the base of the brain and could be experiencing a longer vibration with lower dissipation, which might be the cause of higher harmonics in this region.

To ensure the accuracy and reliability of our modal analysis results on relative displacements, we conducted an additional modal analysis using the maximum principal strain (MPS) values of individual elements within each brain region. This approach provided a more comprehensive understanding of the brain FE model's behavior during helmeted impacts, allowing us to establish a correlation between modal characteristics and MPS values. We validated our relative displacement-based modal analysis results by comparing them to the findings obtained through the MPS-based DMD approach. Our analysis showed a high degree of similarity between the two sets of results, with identical frequencies observed for the main harmonic and a close frequency range for the secondary harmonic. However, we observed some differences when comparing the results based on relative displacement versus MPS. Specifically, in the front impact, the MPS-based results showed a significantly higher amplitude of the second harmonic in the bicycle helmet compared to the relative displacement-based results in the brain. This heightened frequency component could potentially be ascribed to the intrinsic nature of MPS, which has a non-linear relationship with strain. This characteristic might contribute to the emergence of higher harmonics within the MPS-derived modes. Furthermore, we observed that the second oscillation mode in the brainstem of the bicycle helmet occurs at a higher frequency with a higher modal amplitude. This can be attributed to the highest MPS ratio observed in the brainstem for all helmet types during the front impact direction (Fig. 5). Additionally, our examination of the comparative bandwidth modal response among different helmet types at each region showed highly consistent results between the two modal analysis approaches, indicating the reliability and consistency of our findings. Overall, the similarity between the two approaches suggests that our relative-displacement based modal analysis is a highly accurate and reliable method for investigating the dynamical behavior of a simulated human brain model during helmeted impacts.

Considering our hypothesis regarding the helmet's performance in affecting the modal behavior of the regions in this brain model, we expected distinct modal behavior among different helmet types in each region. We found substantial differences in the modal dynamics of the brain model's substructures. In general, the ski and bicycle helmets were less capable of dissipating energy in higher frequencies, compared to the hockey and football helmets for the same frequency range. This was especially evident in the cerebellum, in which in the bicycle and ski helmets, the oscillation at higher frequencies had higher amplitudes. The simulated difference in the modal behavior of the brain structures in this computer model, especially after the ω_{ref}, revealed insight into the effect of the helmets in dissipating energy in higher frequency ranges. To make this reflection quantitatively comparable, we compared the cumulative amplitudes of the frequencies higher than $2\times\omega_{\mathrm{ref}}$. The high-frequency cumulative amplitudes of the ski and bicycle helmets were higher than football and hockey helmets in most cases. The probable explanation for this observation was the difference in the liner material properties of the helmets. The liner foams of the hockey and football helmets that were used were made up PU foam which is softer than EPS foam [5,13,16,105]. Thicker and softer liners make the helmet more effective than soft single layer liners in shock absorption of a broader range of impacts, especially in high velocity impacts [105,106]. On the other hand, the liners of the bicycle and ski helmets are made up of EPS [12–15], which is a stiffer material with more limited bandwidth for dissipation [107]. Moreover, a significant difference in the high-frequency cumulative amplitudes between the bicycle helmet and other helmets in the CC in the front impact might be due the geometrical properties of the bicycle helmet, which has a lower radius of curvature at the front and allows for a lower contact area for front impacts [57]. Another interesting finding was the ability of the football helmet to dissipate high-frequency modes in all regions compared to other helmets for side impacts (Fig. 4A).

Since multimodal behavior of the brain, and the interaction of these modes were found to be associated with peak principal strains [70], we analyzed the relationship between modal amplitude distribution in the high and low frequency regimes and corresponding MPS values (Figs. 4 and 5). Our hypotheses were: (1) A high-frequency cumulative amplitude could be associated with a high MPS in that brain model's substructure, (2) Higher modal density and coupling could lead to higher MPS. Our cumulative amplitude and MPS analyses mainly demonstrated the validity of these points (Figs. 4 and 5). For instance, in the brainstem, ski and bicycle helmets had the highest high-frequency amplitudes, which was in agreement with the strain concentration observed in the MPS analysis (Fig. 5). For cerebellum in the side impacts, ski helmets had the highest high-frequency cumulative amplitude and MPS ratio. For front impacts, football and hockey helmets had the lowest MPS ratio in CC, which was in agreement with the lower high-frequency cumulative modal amplitudes (Fig. 4). Modal coupling and density was also observed to have a substantial effect on strain concentration in this computer model. For instance, although the football helmet for front impacts in cerebellum demonstrated a lower high-frequency cumulative amplitude, it resulted in the highest MPS ratio compared with other helmets. As could be seen in the modal amplitude analysis (Fig. 2), cerebellum demonstrated strong coupling of modes near the main dominant modal frequency. The same observation could be made about the hockey helmet for side impacts in CC, where a strong modal coupling was observed around the main frequency, which could be the reason of increased MPS ratio in CC compared to other helmets.

Our study has multiple limitations that can restrict the broad applicability of our results. The current testing method, which involves a straight impact from a pendulum, does not consider the tangential component of a realistic oblique impact. To address this, performing pendulum impacts with an impactor that has an angled surface could improve simulating real-world scenarios, particularly in terms of their protection ability in rotational kinematics [108]. It would be interesting to study the impact of angled surfaces on different helmet types to measure the rotational energy absorption [108,109]. The findings may demonstrate reveal varying performance for helmets tested with an angled surface compared to those tested with a straight surface. However, it is unlikely that such experiments would yield significantly different dynamic behavior in the frequency domain. Our impact pendulum tests were carried out for one hundred milliseconds, which limited DMD's capability to extract modes with a high-frequency resolution. This might decrease the accuracy of the quantified modal frequencies. However, to tackle this limitation, we also analyzed binned the modes in two frequency ranges to obtain a more global understanding of how the frequency distribution of modes affects the brain response. Prior modal analyses of the brain were either conducted through *in vivo* studies [98], or *in silico* studies with different FE brain models [49,70]. Given the differences in the geometry, pre-defined material properties, and boundary conditions of brain FE models, the frequencies that we observe here might be only applicable to the GHBMC model. For instance, it is important to highlight that the ventricles in the brain contain cerebrospinal fluid (CSF) and therefore must be modeled as fluid structures, the utilized GHBMC head model defines these components as incompressible solid structures with viscoelastic properties. Fluid behavior cannot be accurately simulated using a soft, nearly incompressible solid model, as it may change the mechanical behaviors [110]. Utilizing a computational model that more accurately represents the complex anatomical structures and properties of the brain could potentially result in more precise and accurate predictions of the brain's mechanical response to impacts or other types of loading. Furthermore, we used the isotropic version of the GHBMC head model with the pre-defined material properties that could limit the accuracy of the modal frequencies. In addition, a more comprehensive study on the modal behavior of the helmeted impacts can be achieved by using a more diverse set of helmet designs and impact conditions.

Given the high number of sport-related mTBIs and the potential for improving the performance of sports helmets, this study brings up the importance of considering the dynamical behavior of the brain substructures in designing helmets. Current helmets are designed to mitigate the kinematics of the head, while the brain substructure dynamics play an important role in the concussion mechanism. Moreover, the existence of the localized modes in the brain, and the multimodal behavior of this hyperviscoelastic tissue indicate a necessity for investigating the performance of various helmets in tuning the modal behavior of the brain subregions. The results of this paper can help future studies to expand the research on the dynamical behavior of the brain substructures in more complex loading conditions and wide-ranging helmet types, and eventually, improve helmet designs by providing a design framework relying on brain biomechanics.

Declaration of competing interest

The authors have no conflicts of interest to declare.

Data availability

Data will be made available on request.

Acknowledgments

We would like to acknowledge support from the National Science Foundation (NSF) CMMI awards under Grant Nos. 2145512, and 2227232.

Appendix A. Supplementary data

Supplementary material related to this article can be found online at https://doi.org/10.1016/j.brain.2023.100082.

References

[1] J. Ghajar, Traumatic brain injury, Lancet 356 (9233) (2000) 923–929.

[2] M. McCrea, T. Hammeke, G. Olsen, P. Leo, K. Guskiewicz, Unreported concussion in high school football players: implications for prevention, Clin. J. Sport Med. 14 (1) (2004) 13–17.

[3] J.A. Langlois, W. Rutland-Brown, M.M. Wald, The epidemiology and impact of traumatic brain injury: a brief overview, J. Head Trauma Rehabil. 21 (5) (2006) 375–378.

[4] J.F. Malec, A.W. Brown, C.L. Leibson, J.T. Flaada, J.N. Mandrekar, N.N. Diehl, P.K. Perkins, The mayo classification system for traumatic brain injury severity, J. Neurotrauma 24 (9) (2007) 1417–1424.

[5] M.L. Levy, B.M. Ozgur, C. Berry, H.E. Aryan, M.L. Apuzzo, Birth and evolution of the football helmet, Neurosurgery 55 (3) (2004) 656–662.

[6] R.G. Attewell, K. Glase, M. McFadden, Bicycle helmet efficacy: a meta-analysis, Accid. Anal. Prev. 33 (3) (2001) 345–352.

[7] J. Abderezaei, F. Rezayaraghi, B. Kain, A. Menichetti, M. Kurt, An overview of the effectiveness of bicycle helmet designs in impact testing, Front. Bioeng. Biotechnol. 9 (2021).

[8] M.D. Cusimano, J. Kwok, The effectiveness of helmet wear in skiers and snowboarders: a systematic review, Br. J. Sports Med. 44 (11) (2010) 781–786.

[9] L.R. Scott, S. Bazargan-Hejazi, A. Shirazi, D. Pan, S. Lee, S.A. Teruya, M. Shaheen, Helmet use and bicycle-related trauma injury outcomes, Brain Injury 33 (13–14) (2019) 1597–1601.

[10] J.Y. Sone, D. Kondziolka, J.H. Huang, U. Samadani, Helmet efficacy against concussion and traumatic brain injury: a review, J. Neurosurg. 126 (3) (2017) 768–781.

[11] C.M. Bonfield, S.S. Shin, A.S. Kanter, Helmets, head injury and concussion in sport, Phys. Sportsmed. 43 (3) (2015) 236–246.

[12] P. Rousseau, A. Post, T. Hoshizaki, The effects of impact management materials in ice hockey helmets on head injury criteria, Proc. Inst. Mech. Eng. P 223 (4) (2009) 159–165.

[13] A. Post, A. Oeur, B. Hoshizaki, M.D. Gilchrist, An examination of American football helmets using brain deformation metrics associated with concussion, Mater. Des. 45 (2013) 653–662.

[14] N. Mills, A. Gilchrist, Bicycle helmet design, Proc. Inst. Mech. Eng. L 220 (4) (2006) 167–180.

[15] D. Stewart, L.R. Young, R. Goel, et al., Evaluating the performance of helmet linings incorporating fluid channels, J. ASTM Int. 7 (10) (2010).

[16] D.C. Viano, D. Halstead, Change in size and impact performance of football helmets from the 1970s to 2010, Ann. Biomed. Eng. 40 (1) (2012) 175–184.

[17] T.B. Hoshizaki, S.E. Brien, The science and design of head protection in sport, Neurosurgery 55 (4) (2004) 956–967.

[18] M.L. Bland, Assessing the Efficacy of Bicycle Helmets in Reducing Risk of Head Injury (Ph.D. thesis), Virginia Tech, 2019.

[19] E. Bliven, A. Rouhier, S. Tsai, R. Willinger, N. Bourdet, C. Deck, S.M. Madey, M. Bottlang, Evaluation of a novel bicycle helmet concept in oblique impact testing, Accid. Anal. Prev. 124 (2019) 58–65.

[20] B. Rowson, S. Rowson, S.M. Duma, Hockey STAR: a methodology for assessing the biomechanical performance of hockey helmets, Ann. Biomed. Eng. 43 (10) (2015) 2429–2443.

[21] A. Post, L. Dawson, T.B. Hoshizaki, M.D. Gilchrist, M.D. Cusimano, Development of a test method for adult ice hockey helmet evaluation, Comput. Methods Biomech. Biomed. Eng. 23 (11) (2020) 690–702.

[22] Consumer Product Safety Commission, et al., Safety Standard for Bicycle Helmets; Final Rule, 16 CFR Part 1203, Consumer Product Safety Commission, Bethesda, Maryland, 1998.

[23] NOCSAE, Standard test method and equipment used in evaluating the performance characteristics of protective headgear/equipment, NOCSAE (2013).

[24] M.A. Allison, The performance of helmet-based kinematic measurement systems: Importance for mild traumatic brain injury prevention, 2015.

[25] K. Bian, H. Mao, Mechanisms and variances of rotation-induced brain injury: a parametric investigation between head kinematics and brain strain, Biomech. Model. Mechanobiol. 19 (6) (2020) 2323–2341.

[26] L.F. Gabler, J.R. Crandall, M.B. Panzer, Development of a second-order system for rapid estimation of maximum brain strain, Ann. Biomed. Eng. 47 (9) (2019) 1971–1981.

[27] K. Ghazi, M. Begonia, S. Rowson, S. Ji, American football helmet effectiveness against a strain-based concussion mechanism, Ann. Biomed. Eng. (2022) 1–12.

[28] L.E. Miller, J.E. Urban, M.A. Espeland, M.P. Walkup, J.M. Holcomb, E.M. Davenport, A.K. Powers, C.T. Whitlow, J.A. Maldjian, J.D. Stitzel, Cumulative strain-based metrics for predicting subconcussive head impact exposure–related imaging changes in a cohort of American youth football players, J. Neurosurg.: Pediatr. 29 (4) (2022) 387–396.

[29] M. Goutnik, J. Goeckeritz, Z. Sabetta, T. Curry, M. Willman, J. Willman, T. Currier Thomas, B. Lucke-Wold, Neurotrauma prevention review: improving helmet design and implementation, Biomechanics 2 (4) (2022) 500–512.

[30] A.I. King, K.H. Yang, L. Zhang, W. Hardy, D.C. Viano, Is head injury caused by linear or angular acceleration, in: IRCOBI Conference, Vol. 12, Lisbon, Portugal, 2003.

[31] E.G. Takhounts, V. Hasija, S.A. Ridella, S. Rowson, S.M. Duma, Kinematic rotational brain injury criterion (BRIC), in: Proceedings of the 22nd Enhanced Safety of Vehicles Conference. Paper, no. 11–0263, 2011, pp. 1–10.

[32] S. Rowson, S.M. Duma, Brain injury prediction: assessing the combined probability of concussion using linear and rotational head acceleration, Ann. Biomed. Eng. 41 (5) (2013) 873–882.

[33] K.S. Lota, N. Malliaropoulos, W. Blach, T. Kamitani, A. Ikumi, V. Korakakis, N. Maffulli, Rotational head acceleration and traumatic brain injury in combat sports: a systematic review, Br. Med. Bull. 141 (1) (2022) 33–46.

[34] NOCSAE, National operating committee on standards for athletic equipment. standard performance specification for newly manufactured football helmets, NOCSAE DOC (ND) (2021) 002–17m21.

[35] M.L. Bland, C. McNally, D.S. Zuby, B.C. Mueller, S. Rowson, Development of the STAR evaluation system for assessing bicycle helmet protective performance, Ann. Biomed. Eng. 48 (1) (2020) 47–57.

[36] M. Begonia, A.M. Tyson, B. Rowson, S. Rowson, Hockey STAR methodology, 2020.

[37] F. Abayazid, K. Ding, K. Zimmerman, H. Stigson, M. Ghajari, A new assessment of bicycle helmets: the brain injury mitigation effects of new technologies in oblique impacts, Ann. Biomed. Eng. (2021) 1–18.

[38] T.B. Hoshizaki, A. Post, R.A. Oeur, S.E. Brien, Current and future concepts in helmet and sports injury prevention, Neurosurgery 75 (suppl_4) (2014) S136–S148.

[39] F. Hernandez, L.C. Wu, M.C. Yip, K. Laksari, A.R. Hoffman, J.R. Lopez, G.A. Grant, S. Kleiven, D.B. Camarillo, Six degree-of-freedom measurements of human mild traumatic brain injury, Ann. Biomed. Eng. 43 (8) (2015) 1918–1934.

[40] C. Kuo, L.C. Wu, P.P. Ye, K. Laksari, D.B. Camarillo, E. Kuhl, Pilot findings of brain displacements and deformations during roller coaster rides, J. Neurotrauma 34 (22) (2017) 3198–3205.

[41] X. Zhan, Y. Liu, S.J. Raymond, H.V. Alizadeh, A.G. Domel, O. Gevaert, M. Zeineh, G. Grant, D.B. Camarillo, Deep learning head model for real-time estimation of entire brain deformation in concussion, 2020, arXiv preprint arXiv:2010.08527.

[42] W. Zhao, Y. Cai, Z. Li, S. Ji, Injury prediction and vulnerability assessment using strain and susceptibility measures of the deep white matter, Biomech. Model. Mechanobiol. 16 (5) (2017) 1709–1727.
[43] L.E. Miller, J.E. Urban, E.M. Davenport, A.K. Powers, C.T. Whitlow, J.A. Maldjian, J.D. Stitzel, Brain strain: computational model-based metrics for head impact exposure and injury correlation, Ann. Biomed. Eng. 49 (3) (2021) 1083–1096.
[44] E.G. Takhounts, S.A. Ridella, V. Hasija, R.E. Tannous, J.Q. Campbell, D. Malone, K. Danelson, J. Stitzel, S. Rowson, S. Duma, Investigation of traumatic brain injuries using the next generation of simulated injury monitor (simon) finite element head model, Stapp Car Crash J. 52 (2008) 1.
[45] L.E. Miller, J.E. Urban, J.D. Stitzel, Validation performance comparison for finite element models of the human brain, Comput. Methods Biomech. Biomed. Eng. 20 (12) (2017) 1273–1288.
[46] S. Kleiven, Finite Element Modeling of the Human Head (Ph.D. thesis), KTH, 2002.
[47] S. Ji, H. Ghadyani, R.P. Bolander, J.G. Beckwith, J.C. Ford, T.W. McAllister, L.A. Flashman, K.D. Paulsen, K. Ernstrom, S. Jain, et al., Parametric comparisons of intracranial mechanical responses from three validated finite element models of the human head, Ann. Biomed. Eng. 42 (1) (2014) 11–24.
[48] L.E. Miller, J.E. Urban, J.D. Stitzel, Development and validation of an atlas-based finite element brain model, Biomech. Model. Mechanobiol. 15 (5) (2016) 1201–1214.
[49] K. Laksari, L.C. Wu, M. Kurt, C. Kuo, D.C. Camarillo, Resonance of human brain under head acceleration, J. R. Soc. Interface 12 (108) (2015) 20150331.
[50] S. Ji, M. Ghajari, H. Mao, R.H. Kraft, M. Hajiaghamemar, M.B. Panzer, R. Willinger, M.D. Gilchrist, S. Kleiven, J.D. Stitzel, Use of brain biomechanical models for monitoring impact exposure in contact sports, Ann. Biomed. Eng. (2022) 1–20.
[51] N. Mills, A. Gilchrist, Oblique impact testing of bicycle helmets, Int. J. Impact Eng. 35 (9) (2008) 1075–1086.
[52] K. Hansen, N. Dau, F. Feist, C. Deck, R. Willinger, S.M. Madey, M. Bottlang, Angular Impact Mitigation system for bicycle helmets to reduce head acceleration and risk of traumatic brain injury, Accid. Anal. Prev. 59 (2013) 109–117.
[53] P.A. Cripton, D.M. Dressler, C.A. Stuart, C.R. Dennison, D. Richards, Bicycle helmets are highly effective at preventing head injury during head impact: head-form accelerations and injury criteria for helmeted and unhelmeted impacts, Accid. Anal. Prev. 70 (2014) 1–7.
[54] H. Stigson, M. Rizzi, A. Ydenius, E. Engström, A. Kullgren, Consumer testing of bicycle helmets, in: International Research Council on the Biomechanics of Injury Conference (IRCOBI Conference), Antwerp, Belgium, Sept, 2017, pp. 13–15.
[55] P.G. Petersen, L.V. Smith, D. Nevins, The effect of surface roughness on oblique bicycle helmet impact tests, Proc. Inst. Mech. Eng. P 234 (4) (2020) 320–327.
[56] M. Kurt, K. Laksari, C. Kuo, G.A. Grant, D.B. Camarillo, Modeling and optimization of airbag helmets for preventing head injuries in bicycling, Ann. Biomed. Eng. 45 (4) (2017) 1148–1160.
[57] M.L. Bland, C. McNally, S. Rowson, Differences in impact performance of bicycle helmets during oblique impacts, J. Biomech. Eng. 140 (9) (2018).
[58] M.L. Bland, D.S. Zuby, B.C. Mueller, S. Rowson, Differences in the protective capabilities of bicycle helmets in real-world and standard-specified impact scenarios, Traffic Inj. Prevention 19 (sup1) (2018) S158–S163.
[59] M.L. Bland, C. McNally, S. Rowson, Headform and neck effects on dynamic response in bicycle helmet oblique impact testing, in: Proceedings of the IRCOBI Conference. Athens, Greece, 2018, pp. 413–423.
[60] S.S. Margulies, L.E. Thibault, T.A. Gennarelli, Physical model simulations of brain injury in the primate, J. Biomech. 23 (8) (1990) 823–836.
[61] N. Yoganandan, J. Li, J. Zhang, F.A. Pintar, T.A. Gennarelli, Influence of angular acceleration–deceleration pulse shapes on regional brain strains, J. Biomech. 41 (10) (2008) 2253–2262.
[62] T.M. Abney, Y.A. Feng, R. Pless, R.J. Okamoto, G.M. Genin, P.V. Bayly, Principal components of brain deformation in response to skull acceleration: the roles of sliding and tethering between the brain and skull, in: 26th Southern Biomedical Engineering Conference SBEC 2010, April 30-May 2, 2010, College Park, Maryland, USA, Springer, 2010, pp. 9–12.
[63] E.H. Clayton, G.M. Genin, P.V. Bayly, Transmission, attenuation and reflection of shear waves in the human brain, J. R. Soc. Interface 9 (76) (2012) 2899–2910.
[64] I.E. Kabir, D.A. Caban-Rivera, J. Ormachea, K.J. Parker, C.L. Johnson, M.M. Doyley, Reverberant magnetic resonance elastographic imaging using a single mechanical driver, Physics in Medicine & Biology 68 (5) (2023) 055015.
[65] E. Ozkaya, G. Fabris, F. Macruz, Z.M. Suar, J. Abderezaei, B. Su, K. Laksari, L. Wu, D.B. Camarillo, K.B. Pauly, et al., Viscoelasticity of children and adolescent brains through mr elastography, Journal of the Mechanical Behavior of Biomedical Materials 115 (2021) 104229.
[66] H. Lv, M. Kurt, N. Zeng, E. Ozkaya, F. Marcuz, L. Wu, K. Laksari, D.B. Camarillo, K.B. Pauly, Z. Wang, et al., Mr elastography frequency–dependent and independent parameters demonstrate accelerated decrease of brain stiffness in elder subjects, European radiology 30 (2020) 6614–6623.
[67] M. Kurt, L. Wu, K. Laksari, E. Ozkaya, Z.M. Suar, H. Lv, K. Epperson, K. Epperson, A.M. Sawyer, D. Camarillo, et al., Optimization of a multifrequency magnetic resonance elastography protocol for the human brain, Journal of Neuroimaging 29 (4) (2019) 440–446.
[68] A.K. Knutsen, E. Magrath, J.E. McEntee, F. Xing, J.L. Prince, P.V. Bayly, J.A. Butman, D.L. Pham, Improved measurement of brain deformation during mild head acceleration using a novel tagged mri sequence, Journal of biomechanics 47 (14) (2014) 3475–3481.
[69] S. Kleiven, Evaluation of head injury criteria using a finite element model validated against experiments on localized brain motion, intracerebral acceleration, and intracranial pressure, Int. J. Crashworthiness 11 (1) (2006) 65–79.
[70] K. Laksari, M. Kurt, H. Babaee, S. Kleiven, D. Camarillo, Mechanistic insights into human brain impact dynamics through modal analysis, Phys. Rev. Lett. 120 (13) (2018) 138101.
[71] W. Zhao, S. Ji, White matter anisotropy for impact simulation and response sampling in traumatic brain injury, J. Neurotrauma 36 (2) (2019) 250–263.
[72] J. Abderezaei, W. Zhao, C.L. Grijalva, G. Fabris, S. Ji, K. Laksari, M. Kurt, Nonlinear dynamical behavior of the deep white matter during head impact, Phys. Rev. A 12 (1) (2019) 014058.
[73] E. Gurdjian, V. Hodgson, L. Thomas, L. Patrick, Significance of relative movements of scalp, skull, and intracranial contents during impact injury of the head, J. Neurosurg. 29 (1) (1968) 70–72.
[74] W. Zhao, A. Bartsch, E. Benzel, V. Miele, B.D. Stemper, S. Ji, Regional brain injury vulnerability in football from two finite element models of the human head, in: IRCOBI. Florence, Italy, 2019, pp. 619–621.
[75] A.A. Sabet, E. Christoforou, B. Zatlin, G.M. Genin, P.V. Bayly, Deformation of the human brain induced by mild angular head acceleration, J. Biomech. 41 (2) (2008) 307–315.
[76] J. Escarcega, A. Knutsen, R. Okamoto, D. Pham, P. Bayly, Natural oscillatory modes of 3D deformation of the human brain in vivo, J. Biomech. 119 (2021) 110259.
[77] X. Zhan, Y. Li, Y. Liu, A.G. Domel, H.V. Alizadeh, S.J. Raymond, J. Ruan, S. Barbat, S. Tiernan, O. Gevaert, et al., The relationship between brain injury criteria and brain strain across different types of head impacts can be different, J. R. Soc. Interface 18 (179) (2021) 20210260.
[78] H. Kimpara, M. Iwamoto, Mild traumatic brain injury predictors based on angular accelerations during impacts, Ann. Biomed. Eng. 40 (1) (2012) 114–126.
[79] T.W. McAllister, J.C. Ford, S. Ji, J.G. Beckwith, L.A. Flashman, K. Paulsen, R.M. Greenwald, Maximum principal strain and strain rate associated with concussion diagnosis correlates with changes in corpus callosum white matter indices, Ann. Biomed. Eng. 40 (1) (2012) 127–140.
[80] S. Ji, W. Zhao, J.C. Ford, J.G. Beckwith, R.P. Bolander, R.M. Greenwald, L.A. Flashman, K.D. Paulsen, T.W. McAllister, Group-wise evaluation and comparison of white matter fiber strain and maximum principal strain in sports-related concussion, J. Neurotrauma 32 (7) (2015) 441–454.
[81] Z. Zhou, X. Li, S. Kleiven, Biomechanics of periventricular injury, J. Neurotrauma (2020).
[82] S. Tiernan, A. Meagher, D. O'Sullivan, E. O'Kelly, Finite element simulation of head impacts in mixed martial arts, Comput. Methods Biomech. Biomed. Eng. (2020) 1–11.
[83] H. Mao, L. Zhang, B. Jiang, V.V. Genthikatti, X. Jin, F. Zhu, R. Makwana, A. Gill, G. Jandir, A. Singh, et al., Development of a finite element human head model partially validated with thirty five experimental cases, J. Biomech. Eng. 135 (11) (2013) 111002.
[84] E.G. Takhounts, M.J. Craig, K. Moorhouse, J. McFadden, V. Hasija, Development of brain injury criteria (BrIC), Tech. Rep., SAE Technical Paper, 2013.
[85] A. Alshareef, T. Wu, J.S. Giudice, M.B. Panzer, Toward subject-specific evaluation: methods of evaluating finite element brain models using experimental high-rate rotational brain motion, Biomech. Model. Mechanobiol. 20 (6) (2021) 2301–2317.
[86] A.M. Nahum, R. Smith, C.C. Ward, Intracranial pressure dynamics during head impact, Tech. Rep., SAE Technical Paper, 1977.
[87] X. Trosseille, C. Tarriere, F. Lavaste, F. Guillon, A. Domont, Development of a FEM of the human head according to a specific test protocol, Tech. Rep., SAE technical paper, 1992.
[88] W.N. Hardy, C.D. Foster, M.J. Mason, K.H. Yang, A.I. King, S. Tashman, Investigation of head injury mechanisms using neutral density technology and high-speed biplanar X-ray, Tech. Rep., SAE Technical Paper, 2001.
[89] W.N. Hardy, M.J. Mason, C.D. Foster, C.S. Shah, J.M. Kopacz, K.H. Yang, A.I. King, J. Bishop, M. Bey, W. Anderst, et al., A study of the response of the human cadaver head to impact, Stapp Car Crash J. 51 (2007) 17.
[90] G.W. Nyquist, J.M. Cavanaugh, S.J. Goldberg, A.I. King, Facial impact tolerance and response, SAE Trans. (1986) 850–871.
[91] N. Yoganandan, F.A. Pintar, A. SANCES JR, P.R. Walsh, C.L. Ewing, D.J. Thomas, R.G. Snyder, Biomechanics of skull fracture, J. Neurotrauma 12 (4) (1995) 659–668.
[92] V.R. Hodgson, J. Brinn, L. Thomas, S. Greenberg, Fracture behavior of the skull frontal bone against cylindrical surfaces, Tech. Rep., SAE Technical Paper, 1970.

[93] P.J. Schmid, Dynamic mode decomposition of numerical and experimental data, J. Fluid Mech. 656 (2010) 5–28.
[94] M. Grilli, P.J. Schmid, S. Hickel, N.A. Adams, Analysis of unsteady behaviour in shockwave turbulent boundary layer interaction, J. Fluid Mech. 700 (2012) 16–28.
[95] L.F. Gabler, H. Joodaki, J.R. Crandall, M.B. Panzer, Development of a single-degree-of-freedom mechanical model for predicting strain-based brain injury responses, J. Biomech. Eng. 140 (3) (2018) 031002.
[96] Y. Liu, X. Zhan, A.G. Domel, M. Fanton, Z. Zhou, S.J. Raymond, H.V. Alizadeh, N.J. Cecchi, M. Zeineh, G. Grant, Theoretical and numerical analysis for angular acceleration being determinant of brain strain in mTBI, 2020, arXiv preprint arXiv:2012.13507.
[97] M. Hajiaghamemar, S.S. Margulies, Multi-scale white matter tract embedded brain finite element model predicts the location of traumatic diffuse axonal injury, J. Neurotrauma 38 (1) (2021) 144–157.
[98] A.K. Knutsen, A.D. Gomez, M. Gangolli, W.-T. Wang, D. Chan, Y.-C. Lu, E. Christoforou, J.L. Prince, P.V. Bayly, J.A. Butman, et al., In vivo estimates of axonal stretch and 3D brain deformation during mild head impact, Brain Multiphys. (2020) 100015.
[99] D. Bradshaw, J. Ivarsson, C. Morfey, D.C. Viano, Simulation of acute subdural hematoma and diffuse axonal injury in coronal head impact, J. Biomech. 34 (1) (2001) 85–94.
[100] L. Zhang, K.H. Yang, A.I. King, Comparison of brain responses between frontal and lateral impacts by finite element modeling, J. Neurotrauma 18 (1) (2001) 21–30.
[101] J. Ho, Z. Zhou, X. Li, S. Kleiven, The peculiar properties of the falx and tentorium in brain injury biomechanics, J. Biomech. 60 (2017) 243–247.
[102] A. Macpherson, A. Spinks, Bicycle helmet legislation for the uptake of helmet use and prevention of head injuries, Cochrane Database Syst. Rev. (3) (2008).
[103] A. Jesudoss, R. Vybhavi, B. Anusha, Design of smart helmet for accident avoidance, in: 2019 International Conference on Communication and Signal Processing (ICCSP), IEEE, 2019, pp. 0774–0778.
[104] T. Wu, J. Antona-Makoshi, A. Alshareef, J.S. Giudice, M.B. Panzer, Investigation of cross-species scaling methods for traumatic brain injury using finite element analysis, J. Neurotrauma 37 (2) (2020) 410–422.
[105] A. Subic, Materials in Sports Equipment, Woodhead Publishing, 2019.
[106] W.C. Moss, M.J. King, E.G. Blackman, Towards reducing impact-induced brain injury: lessons from a computational study of army and football helmet pads, Comput. Methods Biomech. Biomed. Eng. 17 (11) (2014) 1173–1184.
[107] F. Shuaeib, A. Hamouda, S. Wong, R.R. Umar, M.M. Ahmed, A new motorcycle helmet liner material: The finite element simulation and design of experiment optimization, Mater. Des. 28 (1) (2007) 182–195.
[108] M. Aare, P. Halldin, A new laboratory rig for evaluating helmets subject to oblique impacts, Traffic Inj. prevention 4 (3) (2003) 240–248.
[109] P. Halldin, S. Kleiven, The development of next generation test standards for helmets, in: 1st International Conference on Helmet Performance and Design, Vol. 1, 2013.
[110] M. McGarry, E. Van Houten, D. Sowinski, D. Jyoti, D.R. Smith, D.A. Caban-Rivera, G. McIlvain, P. Bayly, C.L. Johnson, J. Weaver, et al., Mapping heterogenous anisotropic tissue mechanical properties with transverse isotropic nonlinear inversion MR elastography, Med. Image Anal. 78 (2022) 102432.